

Original Article

Nitrite exposure may induce infertility in mice

Shanshan Wu^{1,4a}, Sang Hu^{2a}, Wenjuan Fan³, Xiaojing Zhang¹, Haili Wang¹, Chaojie Li¹, and Jinbo Deng^{1*}

¹ National Health Commission Key Laboratory of Birth Defects Prevention, Henan Key Laboratory of Population Defects Prevention, Henan Institute of Reproduction Health Science and Technology, 26 Jingwu Road, Zhengzhou 450002, China

² Fourth Affiliated Hospital of Anhui Medical University, Hefei, Anhui Province, China

³ Luohe Medical College, Luohe City, Henan Province, China

⁴ Third Affiliated Hospital of Zhengzhou University, Zhengzhou, Henan Province, China

Abstract: In the present study, we investigated the potential of nitrite exposure to induce infertility in mice. Adult female C57BL/6J mice were randomly divided into control and nitrite exposure groups. Subsequently, the rate of mouse infertility was calculated, and pathological changes in ovarian tissues were examined using hematoxylin and eosin staining. In addition, TUNEL staining, immunofluorescent labeling, and western blotting were performed to assess cell apoptosis and oxidative stress response in ovarian tissues from various groups. We observed that nitrite exposure could induce infertility ($p < 0.05$) in mice. High-dose nitrite exposure caused infertility in a time-dependent manner, and two-round exposure induced higher infertility than that one-round exposure ($p < 0.01$). In addition, a higher number of atretic follicles were detected in the ovaries of nitrite-exposed groups than in the control group. Furthermore, TUNEL-positive cells were observed in granulosa cells of atretic follicles, and overexpression of caspase 8, c-Fos, and inducible nitric oxide synthase (iNOS) was detected in ovaries after nitrite exposure ($p < 0.01$), suggesting that cell apoptosis and oxidative stress response were induced following nitrite exposure. Collectively, these findings suggest that nitrite exposure can induce mouse infertility in a time-dependent manner. Oxidative stress response and cell apoptosis are involved in mediating nitrite-induced infertility. (DOI: 10.1293/tox.2021-0002; J Toxicol Pathol 2022; 35: 75–82)

Key words: atretic follicle, cell apoptosis, infertility, nitrite exposure, oxidative stress response

Introduction

Nitrite is an inorganic chemical compound that is often used as an additive for food preservation. Given its ability to inhibit microorganisms, including *Bacillus* and *Clostridium botulinum*, nitrite is frequently used in meat processing¹. However, excessive nitrite can be toxic, potentially inducing acute and chronic poisoning. Acute nitrite poisoning can cause urgent and notable symptoms, including abdominal pain, nausea, vomiting, diarrhea, and methemoglobinemia. Chronic poisoning can cause permanent, even undetectable, damage to the body. Chronic poisoning can damage multiple systems and organs, including the nervous, immune, and digestive systems, and possible carcinogenic and teratogenic effects². In addition to food additives, nitrite exposure

can occur through the drinking water, especially chronic nitrite poisoning. Industrial waste pollution is an important source of nitrite in drinking water. Given its potential to harm human health, countries have stipulated nitrite standards for drinking water and food. For example, in China, the hygienic standards for food additives in meat products mandate that nitrite levels should not exceed 0.15 mg/kg. Furthermore, according to the US National Environmental Protection Agency and regulatory agencies in the European Union (EU), <1 mg/L and 0.5 mg/L nitrite should be present in drinking water, respectively.

Studies examining nitrite toxicity have mainly focused on the mechanism of acute nitrite poisoning and its clinical treatment owing to the urgency of acute poisoning symptoms. More recently, researchers have focused on chronic nitrite poisoning, given its potential for severely impacting human health. Our previous studies have revealed that nitrite can cause mental retardation and developmental delay in the central nervous system, especially dendritic development³. Moreover, nitrite toxicity can reportedly impact other functions^{4–8}. For example, considering reproduction and infertility, nitrite can cross the placenta and induce fetal abortion^{9, 10}. However, previous studies on nitrite-induced infertility are limited and warrant additional experimental evidence to comprehensively elucidate underlying mecha-

Received: 8 January 2021, Accepted: 26 October 2021

Published online in J-STAGE: 4 December 2021

*The first two authors contributed equally to this work.

*Corresponding author: J Deng (e-mail: jinbo_deng2017@126.com)

©2022 The Japanese Society of Toxicologic Pathology

This is an open-access article distributed under the terms of the Creative Commons Attribution Non-Commercial No Derivatives

(by-nc-nd) License. (CC-BY-NC-ND 4.0: <https://creativecommons.org/licenses/by-nc-nd/4.0/>).



nisms. In the present study, we examined nitrite exposure-induced infertility in mice. Additionally, we examined apoptosis in follicular granulosa cells. Furthermore, we attempted to elucidate potential mechanisms underlying nitric oxide (NO)-activated oxidative stress response and apoptosis pathways. Accordingly, our study will generate further data regarding the impact of nitrite toxicity on the reproductive system, as well as provide valuable information to guide hygiene standards for food and water.

Materials and Methods

Animals

Healthy adult male and female C57BL/6J mice were provided by the Experimental Animal Center of the Henan Institute of Reproduction Health Science and Technology. All experiments were performed in accordance with the guidelines and approval of the Animal Welfare and Use Committees of the Institute to ensure animal welfare during the experiments. Adult male and female mice were housed in standard breeding cages (each cage housed one male and two females) with a 12/12-h light/dark cycle. For experiments, female mice older than P30 (postnatal day 30) were employed, given that mice attain reproductive ability at P30. The youngest males and females were mated at P30; however, natural conception until after P40 was preferable. Given the different pregnancy times, precise age at pregnancy and sacrifice could not be determined. In principle, the age at pregnancy for round one exposure was P40–P100, whereas the age at round two exposure ranged between P90–P160 (see also graphical abstract). In housed cages, 2–5 month-old mating males were often replaced to accelerate female pregnancy. Females were checked each morning for a vaginal plug; the day at which a positive plug was observed was termed G0 (gestation day 0). Pups (usually 5–10 mice in each nest) were born from timed pregnancies at gestational day 19. The animals were housed in a clean environment at 22–25°C, with a relative humidity of 50–60% and free access to food and water. Female mice were randomly divided into control and nitrite exposure groups. The females in the control group received a daily intragastric gavage of normal saline (0.02 mL/kg) from G0 until pup birth. Four hours be-

fore gavage, animals were deprived of water and food. In addition, nitrite exposure groups were established. Nitrite doses were defined based on the concentration of human acute food poisoning and mouse tolerance for nitrite. Based on the nitrite exposure time and dose, mice were divided into four groups: (1) low dose with one round (once gestation period) of nitrite exposure = low-dose nitrite (60 mg/kg in saline) + one pregnancy cycle gavage (from G0 to pup birth) (Chen *et al.*, 2016); (2) high-dose with one round (once gestation period) of nitrite exposure = high dose nitrite (120 mg/kg in saline) + one pregnancy cycle gavage (from G0 to pup birth). After completion of pregnancy and lactation, a few mice were subjected to another round of gestation and nitrite exposure. The dams were housed with male mice, and vaginal plugs were checked each morning as performed earlier. Low-dose and high-dose round-two nitrite exposure was performed. For instance, (3) low dose with two rounds (twice gestation) nitrite exposure = low-dose nitrite (60 mg/kg in saline) + two pregnancy cycles of nitrite gavage. Like the first gestation, the second exposure was initiated from G0 to pup birth. (4) High-dose with two rounds (twice gestation) nitrite exposure = high-dose nitrite (120 mg/kg in saline) + two pregnancy cycle gavage. In the control group, water and food were withheld for 4 h before gavage. Finally, the infertility rate was calculated among various groups, and females who failed to achieve pregnancy after mating continuously for at least 2 months were defined as cases of infertility. Table 1 shows experimental cases and infertile mice in various experimental groups. Animals from different groups were selected and sacrificed at defined time points; for instance, the fertile dams were sacrificed after weaning, and the infertile dams were sacrificed after more than two months without pregnancy. After observing infertility, the dams were sacrificed, and the ovaries were harvested for further pathological and biochemical analyses. The following cases were used to ensure statistical tests: hematoxylin-eosin (H&E) staining (at least 10 cases in each group), immunocytochemistry (at least 10 cases in each group), TUNEL staining (at least 5 cases in each group), and western blotting (at least 5 cases in each group).

Table 1. Infertility Rates in Various Experimental Groups

	Control group (A)	Low dose with one round nitrite exposure (B)	High dose with one round nitrite exposure (C)	Low dose with two round nitrite exposure (D)	High dose with two round nitrite exposure (E)
Infertility vs. total number	2/66	8/32	14/32	14/24	16/18
Infertility rate	3.03%	25.00%*	43.75%*	58.33%*	88.89%*, **

A: control group; B: low dose group with one round of nitrite exposure; C: high dose group with one round of nitrite exposure; D: low dose group with two rounds of nitrite exposure; E: high dose groups with two rounds of nitrite exposure. Using the χ^2 test, various groups were compared. *: $p < 0.01$, if compared with control. **: $p < 0.01$, if compared with low dose nitrite with one round of exposure (B and E). The following are details of pairwise comparison: B vs. A (*), C vs. A (*), C vs. B, D vs. A (*), D vs. B, D vs. C, E vs. A (*), E vs. B (**), E vs. C, E vs. D, respectively. The tests indicate statistical differences between control and nitrite exposure groups. The high dose shows a statistically significant difference in the rate of infertility after one vs. two rounds of nitrite exposure, indicating an enhanced effect upon repeated exposure.

Hematoxylin and eosin staining

In brief, ovaries were harvested from control and treatment groups and were then subjected to routine procedures, including fixation, dehydration, transparency, paraffin embedding, and sectioning (5- μ m thick sections). The sections were washed with 0.01 M phosphate buffer (0.01 M PB) and stained with H&E for a few minutes. Next, the sections were rinsed with distilled water three times. After gradient dehydration in ethanol (50%, 75%, 95% and 100%), transparency in xylene, and application of coverslip, sections were visualized and photographed using a microscope (BX61; Olympus).

Immunocytochemistry

After ovarian sections were dewaxed, the antigens were repaired by microwave oven heating. Then, sections were rinsed with 0.01 M PB, and nonspecific antigens were blocked with 10% normal goat serum (with 0.3% Triton X-100 and 1% BSA in 0.01 M PB) for 30 min. The sections were incubated overnight with primary antibodies at 4°C. After rinsing three times, sections were incubated with secondary antibodies for 3 h at room temperature. The primary antibody used was mouse anti-iNOS (inducible nitric oxide synthase) monoclonal antibody (1:500, Santa Cruz, SC-7271). The secondary antibody was Alexa Fluor 488 donkey anti-mouse IgG (1:500; Invitrogen, A10037). The negative control was prepared using 0.01 M PB (instead of the primary antibody). Sections were coverslipped with 65% glycerol+300 nM DAPI (D1306, Invitrogen) in PB. DAPI was used to counterstain nucleic acids in cellular nuclei. Finally, sections were imaged with an epifluorescent microscope (BX61, Olympus, Japan) with excitation of ultraviolet or fluorescein isothiocyanate (FITC). High-quality sections were photographed using an Olympus laser confocal microscope (FV1000, Olympus, Japan).

TUNEL fluorescent staining

Terminal deoxynucleotidyl transferase-mediated dUTP-biotin nick end labeling (TUNEL) is a reliable indicator of apoptosis. When cells undergo apoptosis, endogenous endonucleases are activated, and DNA double-strands in the nucleus are broken with exposed 3'-OH ends. Using TUNEL staining, the 3'-OH can be catalyzed and linked by terminal deoxynucleotidyl transferase (TdT), which is combined with fluorescein (FITC)-labeled dUTP (fluorescein-dUTP). Therefore, apoptotic cells exposed to 3'-OH ends are labeled with FITC. Accordingly, TUNEL assay can be used to detect apoptosis by microscopy or flow cytometry. Herein, 5- μ m thick ovarian tissue sections were dewaxed and digested with proteinase K. Sections were then incubated in a solution containing rTdT and fluorescein-dUTP mix reaction liquid (Promega, TB235) at 37°C for 1 h in the dark. The chemical reaction was terminated using 2 \times SSC buffer at room temperature for 15 min. Finally, sections were rinsed with 0.01 M PB and coverslipped with 65% glycerol and 300 nM DAPI. Images were obtained under a fluorescent microscope, as described above.

Western blot analyses for caspase-8 and c-Fos

To further verify cell apoptosis and oxidative stress response in atretic follicles, activated protein caspase-8 and c-Fos were determined in ovarian tissues using western blotting. Mice were sacrificed by cervical dislocation, and the ovaries were quickly dissected and placed in a homogenizer. After homogenization, the ovarian cytoplasmic proteins were extracted using a cytoplasmic protein extraction kit (Shanghai Biyuntian Biotechnology Co., Ltd., P0027). Protein concentrations in samples were measured, subjected to electrophoresis, and transferred to membranes. Then, immune reactions, enzyme labeling, and film exposure were performed sequentially. The primary antibodies, rabbit anti-active caspase-8 polyclonal antibody (1:2,000, Imgenex, IMG5703) and rabbit anti-c-Fos polyclonal antibody (1:1000, Abcam, AB7693), were incubated at 4°C overnight. The secondary antibody, horseradish peroxidase-labeled goat anti-rabbit IgG (1:1000, Beyotime Institute of Biotechnology, A0208), was incubated at room temperature for 1 h. Finally, membranes were incubated in the ECL reagent for 3 min, and X-ray films were exposed. β -actin (Beyotime Institute of Biotechnology, AA128) was used as an internal reference. The grayscale ratio is the relative gray value of target bands versus internal reference bands.

Statistical analyses

Parameter measurements and calculations: (1) infertility rate was calculated using the following formula: infertility rate = number of infertile dams/total dams in each group. In addition, semi-quantitative protein analysis was performed. The gray values of caspase-8 and c-Fos (western blot) were measured using ImageJ software (National Institutes of Health, Bethesda, MD, USA), and β -actin was used as an internal reference. (2) The gray value of protein was calculated from the gray value of the target band/gray value of β -actin.

Statistical analyses: To determine the infertility rate, the χ^2 test was used to compare significance among various groups (Table 1). For semi-quantitative protein analysis, one-way ANOVA was performed among various groups using SPSS 11.5 software (IBM Corp, Chicago, IL, USA). Statistical significance was set at $p < 0.05$. Both control and treatment groups included infertile and non-infertile mice; however, ovaries were not separately examined, owing to minor histological differences among mice in the same group. Thus, we primarily aimed to compare differences between control and treatment groups.

Results

Nitrite exposure and mouse infertility

In the present study, we calculated the infertility rates for various experimental groups. The control group exhibited an infertility rate of 3.03% (2/66), while infertility rates after one round of nitrite exposure were 25.00% (8/32) and 43.75% (14/32) in the low- and high-dose groups, respectively. After round two of nitrite exposure, the infer-

tility rates were 58.33% (14/24) and 88.89% (16/18) in the low- and high-dose groups, respectively (Table 1). Statistical analysis revealed that infertility rates were higher in the nitrite exposure groups than in the control group ($p < 0.01$). For instance, infertility rates in all exposure groups were higher than those in the control group. Moreover, the infertility rate was higher after two rounds of nitrite exposure than after one round of high dose exposure ($p < 0.01$), suggesting that nitrite-induced infertility was time-dependent. In addition, the number of newborn pups was higher in the control group than in the treatment groups. In the control group litter, the number of pups ranged between 5 and 10; in treatment groups, the number of pups ranged between 3 to 7.

Nitrite exposure and cell apoptosis in ovary

Pathological alterations in the ovaries were examined to clarify the underlying cause of nitrite exposure-induced infertility in mice. Following H&E staining under low magnification, we observed that ovaries in the treatment groups were notably atrophied, and blood vessels were congested when compared with the control group (Fig. 1A and 1B). Under high magnification, control group ovaries exhibited follicles at different developmental stages, such as primordial follicles, growing follicles (including primary and secondary follicles), and mature follicles (Fig. 1C and 1D). Typically, in the growing follicle, the oocyte is surrounded by several layers of granulosa cells. As the follicle matures, a cavity appears within the stratum granulosum to form an antral follicle, and finally, a large cavity develops in the Graafian follicles. Herein, we observed some atretic follicles inside the ovary that were degenerative growing follicles with morphological deformations such as oocyte lysis, zona pellucida collapse, follicular wall collapse, and irregular follicle shape (Fig. 1C and 1E). The control group also displayed corpora lutea with loose connective tissue and vessels (Fig. 1D). Following nitrite exposure, the number of growing follicles, including antral follicles and corpora lutea, was reduced; however, the number of atretic follicles was elevated when compared with that in the control group. In treatment groups, almost all follicles were atretic follicles (Fig. 1E). The numbers of atretic follicles and corpora lutea in ovaries were semi-quantitatively analyzed between control and nitrite exposures, and the results are shown in Table 2. Increased atretic follicles and decreased corpora lutea were more pronounced in infertility cases in the high-

dose group than in the low-dose and control groups. Among groups subjected to two rounds of nitrite exposure, the observed lesions were comparable between animals (infertility or fertility) in the low-dose groups and infertile animals in the high-dose groups. Moreover, the lesions in infertile animals in the high-dose groups were more notable than in fertile animals (Table 2).

As atretic follicles are degenerative structures, cell apoptosis has been suggested to inevitably occur in granulosa cells and oocytes¹¹. To further understand cell apoptosis in atretic follicles, TUNEL staining with DAPI counterstaining was performed (Fig. 1F and 1G). In the control group, only a few TUNEL-positive cells were detected among granulosa cells (Fig. 1F); however, a high number of apoptotic cells were observed in the granulosa cells of atretic follicles following nitrite exposure (Fig. 1G). Western blot assays supported the results of TUNEL staining. Based on the semi-quantitative analysis, we detected overexpression of caspase-8 in the treatment group ovarian tissues. For instance, the relative expression level of activated-caspase-8 (0.523 ± 0.09) was higher in the nitrite exposure group (two rounds of high dose exposure) than in the control group (0.316 ± 0.08) (Fig. 2; $p < 0.01$). These results suggested that the apoptosis pathway might be involved in the mechanism underlying nitrite exposure-induced infertility.

Nitrite exposure and oxidative stress response

Theoretically, nitrite and its metabolic product, NO, are strong oxidants of oxidative stress, and c-Fos is a markedly sensitive biomarker for oxidative stress response. In the present study, c-Fos was overexpressed in the nitrite-exposed groups. The relative expression of activated c-Fos was higher in the ovaries of the nitrite exposure group (0.48 ± 0.04 ; exposed twice at the high dose) than that in the control group (0.275 ± 0.07) (Fig. 2; $p < 0.01$), suggesting that oxidative stress response occurred after nitrite exposure. Nitrite can be converted into NO when metabolized, and NO is likely to participate in the activation of the oxidative stress response. Accumulated clinical evidence suggests that high NO concentrations could cause polycystic ovary and endocrine dysfunction of the corpus luteum, leading to female infertility¹². To test this hypothesis, the NO level in the ovary was measured indirectly. As NO is an unstable substance, precise measurement can be challenging. However, the iNOS quantity can be used to infer NO levels indi-

Table 2. Atretic Follicles and Corpora Lutea between Control and Nitrite Exposure Groups

Histopathological examination		Control		60 mg/kg/day (two round)		120 mg/kg/day (two round)	
		Non-infertility	Infertility	Non-infertility	Infertility	Non-infertility	Infertility
Increase	Number of animal examined	64	2	10	14	2	16
atretic follicle	Primary and secondary follicle	Normal	Normal	+	+	+	++
	Antral follicle	Normal	Normal	+	+	+	++
Decrease	corpus luteum	Normal	Normal	-	-	-	--

Mark: normal, normal number; +, slight increased; ++, considerably increased; -, slight decreased; --, considerably decreased. It should be noted that these were observational data, as cases of non-infertility in the high dose group were insufficient to perform statistical analysis.

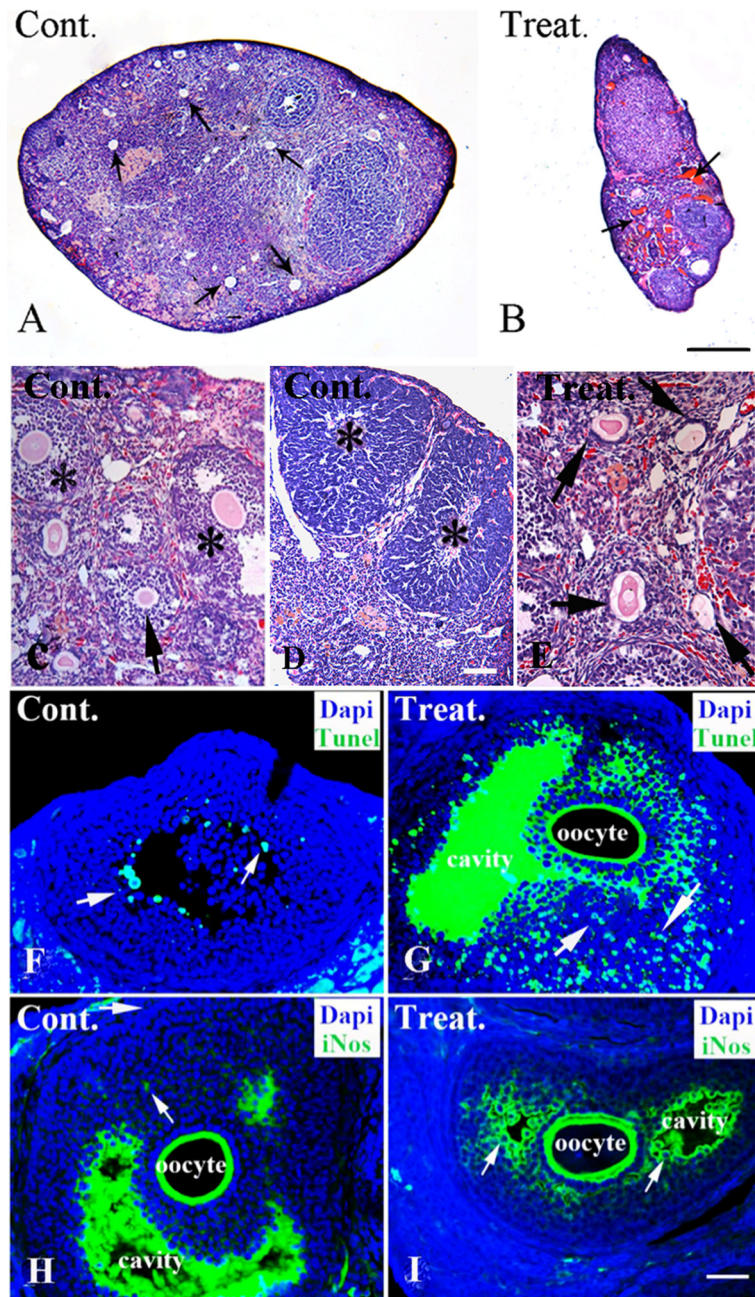


Fig. 1. Pathological and chemical changes in ovaries after nitrite exposure. A–E; Pathological alterations in control and treatment groups (H&E staining). A–B: Low magnification of control and treatment ovaries. The control ovary is plump, with some developing follicles (A, arrow). Conversely, the treatment group ovary shows notable atrophy and congested blood vessels (B, arrow). C–E: High magnification of control and treatment ovaries. Various follicles, including secondary follicles (arrow) and some antral follicles (*), can be observed in the control ovary (C). Corpora lutea with loose connective tissue and vessels inside can be observed in the control group tissues (D, *). After nitrite exposure, mature follicles are decreased, but atretic follicles with morphological deformation (arrow), such as oocyte autolysis, zona pellucida collapse, follicular wall collapse, are markedly increased (E). F–G: Nitrite exposure and cell apoptosis in granulosa follicular cells (TUNEL staining and DAPI counterstaining). In the control group, DAPI counterstaining (blue) shows numerous granulosa cells (blue) surrounding oocytes in the follicles, with few apoptotic cells (green, arrow) in granulosa cells (F). After high-dose nitrite exposure, numerous apoptotic cells (arrow) can be observed in granulosa cells (G). Interestingly, the matrix in the follicular cavity appears to be TUNEL-positive. H–J: Nitrite exposure and iNOS expression in granulosa cells (iNOS immunofluorescent labeling and DAPI counterstaining). In the control group (H), few iNOS positive cells with weak fluorescence (arrow) can be seen in granulosa cells (blue). The matrix in the follicular cavity exhibits iNOS-positivity. After nitrite exposure, numerous iNOS positive cells (arrow) can be observed in follicular granulosa cells (J). It should be noted that although there the iNOS positive matrix in the follicular cavity of the control group is dense, the iNOS positive granulosa cells are few. In contrast, the iNOS positive granulosa cells are enriched in treatment groups (arrow, with DAPI and iNOS double labeling). The control and high-dose exposure groups are indicated as Cont. and Treat. in the upper-left corner, respectively. Scale bar: A-B, 20 μ m; C & E, 50 μ m; D, 100 μ m; F-J, 200 μ m. H&E, hematoxylin-eosin; NOS, nitric oxide synthase; iNOS, inducible nitric oxide synthase.

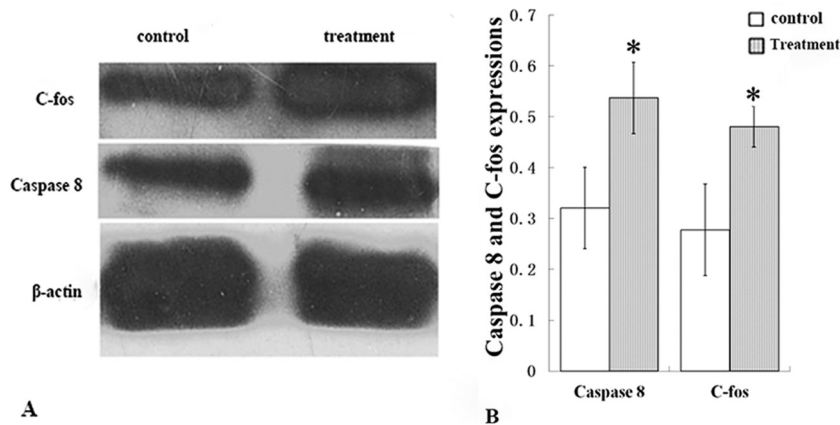


Fig. 2. Western blotting of activated-caspase-8 and c-Fos expressions in ovaries of various experimental groups. Nitrite exposure increases the expression of activated-caspase-8 and c-Fos in ovaries (A). The histogram shows that the differential expressions of caspase-8 and activated c-Fos in the control and high dose exposure group were statistically significant. The grayscale ratio is the relative gray value of target bands vs. internal reference bands, where β -actin was used as the internal reference. Mean \pm standard deviation (SD), $n=5$. *: $p<0.01$, if treatment vs. control.

rectly. NOS is a key enzyme in NO metabolism, and iNOS is a subtype of NOS. In the present study, iNOS expression levels were determined using immunocytochemistry. The results revealed that nitrite exposure increased the number of iNOS-positive granulosa cells with strong fluorescence when compared with the control (Fig. 1F and 1G), indicating that NO activated the oxidative stress response in nitrite exposure groups. Moreover, the matrix in the follicular cavity exhibited TUNEL- and iNOS-positivity; however, the underlying mechanism was unclear, warranting further investigations.

Discussion

Epidemiological studies have shown a correlation between the nitrite concentration in drinking water and spontaneous abortion, and pregnant women in regions with higher nitrate concentrations in drinking water typically experienced higher abortion rates than in other regions¹³. In addition, pregnant women with nitrite-induced miscarriage exhibit a high incidence of methemoglobinemia¹⁴. Although epidemiological studies have suggested that nitrite exposure may contribute to infertility, additional data accumulation is crucial to clarify the mechanism of nitrite-induced infertility. In the present study, we aimed to confirm whether nitrite exposure can induce mouse infertility with dose and repeated-exposure dependency. In addition, we aimed to elucidate whether the oxidative stress response and cell apoptosis mediate infertility induction.

Our results revealed that nitrite exposure could lead to mice infertility when compared with control. Moreover, after two rounds of nitrite exposure, the infertility rate was significantly higher than observed after one round of exposure at high-dose treatment, thus indicating that a repeated-exposure effect can be observed with high-dose treatment. In contrast, the infertility rate in the high-dose group was higher than that in the low-dose group, both with one-round

and two-rounds of nitrite exposure, although the difference was not statistically significant ($p>0.05$). Therefore, increasing the number of experimental animals could help demonstrate dose dependency with statistical significance between one-round exposure and two-round exposures in the high-dose group. Based on pathological observations, nitrite exposure can also induce the degeneration of growing follicles, resulting in atretic follicles with numerous apoptotic cells. The corpora lutea is greatly reduced owing to the increase in atretic follicles. In the present study, cell apoptosis was probably caused by nitrite-induced follicle degeneration and animal infertility. Apoptosis in granulosa cells occurs via the mitochondrial pathway, and caspase family proteins, such as caspase-8 and caspase-3, are activated during the process^{15–17}, as confirmed in the present study. As ovaries in nitrite-treated groups displayed an increase in atretic follicles and a decrease in corpora lutea, this ovarian status resulted in fewer newborn pups, leading to nitrite-induced infertility.

In the present study, the nitrite exposure groups exhibited oxidative stress response in ovarian tissues; oxidative stress is known to promote overexpression of c-Fos (a sensitive monitor of oxidative stress). Western blot semi-quantitative analysis revealed that the c-Fos protein was overexpressed in the ovary following nitrite exposure, demonstrating a further enhanced effect with repeated exposure. Furthermore, NO, an active oxidant, activates and participates in the oxidative stress response. As NOS, especially iNOS, is a key enzyme in NO metabolism and the NO pathway, iNOS can be used to evaluate NO levels indirectly. We observed that nitrite exposure promoted iNOS overexpression in ovaries, suggesting that NO activates the oxidative stress response. Therefore, we can infer that the oxidative stress response contributes to cell apoptosis, as well as nitrite-induced infertility. However, the relationship between the apoptosis pathway and oxidative stress response needs to be elucidated. In addition, the precise interaction between

the NO-activated oxidative stress response and the apoptotic pathway should be examined.

The key molecule, NO, is possibly involved in activating the oxidative stress response and cell apoptosis. NO is important for physiological functions. Ideal NO levels are advantageous for body functions and are considered therapeutic in certain diseases, such as follicular dysplasia. In contrast, high NO levels can activate cell apoptosis and cause functional disorders associated with progesterone and steroids, resulting in follicular degeneration^{18–20}. Lastly, progesterone and steroid disorders can cause implantation failure of fertilized eggs^{21,22}. Thus, NO can also activate the oxidative stress response, and excessive NO inhibits follicular maturation and egg ovulation, resulting in mouse infertility. The NO-activated oxidative stress response can impact the cell apoptosis pathway via reactive oxygen species (ROS). The oxidative stress response can cause ROS accumulation, which in turn causes cell apoptosis. Three types of ROS, peroxide ($O_2^{\cdot -}$), hydrogen peroxide (H_2O_2), and hydroxyl (OH^{\cdot}), are known to exist in the body. Therefore, ROS are toxic to cells and tissues^{23–26}. ROS can maintain balance with antioxidant substances. Superoxide dismutase (SOD) is a typical antioxidant that can eliminate excessive ROS in cells. Once the balance is disrupted, excessive ROS can damage cells, tissues, and even the reproductive system, thus resulting in diseases such as endometriosis and ovarian disorders^{27,28}. In addition, previous studies have shown that H_2O_2 can interfere with gonadotropin and progesterone release^{29,30}. These hormones are important for regulating oocyte development and maturation³¹. Therefore, NO is a key molecule during the oxidative stress response and can be implicated in ovarian cell apoptosis and nitrite-induced infertility in mice.

In summary, (1) nitrite exposure can cause infertility in mice, exhibiting additional effects upon repeated exposure. (2) After nitrite exposure, pathological and chemical changes occur in the ovaries. For instance, atretic follicles and their apoptotic granulosa cells are markedly increased, and iNOS, c-Fos, and caspase-8 are overexpressed in treatment groups, indicating that cell apoptosis and NO-activated oxidative stress response mediate nitrite-induced infertility. (3) Our study may provide useful scientific data to help guide hygienic standards for water and food.

Disclosure of Potential Conflicts of Interest: The authors declare no competing interests.

Acknowledgments: This study was funded by the Medical Science and Technology Project of Henan Provincial Health Commission (LHGJ20190828, LHGJ20190827), Scientific and Technical Project of Henan Science and Technology Department (192102310134), Open Project of National Health Commission Key Laboratory of Birth Defect Prevention (ZD201903), and the Medical Foundation of Health and Family Planning Commission of Henan Province (No. 2018020589).

References

1. Sindelar JJ, and Milkowski AL. Human safety controversies surrounding nitrate and nitrite in the diet. *Nitric Oxide*. **26**: 259–266. 2012. [[Medline](#)] [[CrossRef](#)]
2. Chiu HF, Tsai SS, and Yang CY. Nitrate in drinking water and risk of death from bladder cancer: an ecological case-control study in Taiwan. *J Toxicol Environ Health A*. **70**: 1000–1004. 2007. [[Medline](#)] [[CrossRef](#)]
3. Chen Y, Cui Z, Wang L, Liu H, Fan W, Deng J, and Deng J. The impairment of learning and memory and synaptic loss in mouse after chronic nitrite exposure. *Environ Toxicol*. **31**: 1720–1730. 2016. [[Medline](#)] [[CrossRef](#)]
4. Omar SA, and Webb AJ. Nitrite reduction and cardiovascular protection. *J Mol Cell Cardiol*. **73**: 57–69. 2014. [[Medline](#)] [[CrossRef](#)]
5. Azevedo AMM, Brites-Anselmi G, Pinheiro LC, de Almeida Belo V, Coeli-Lacchini FB, Molina CAF, de Andrade MF, Tucci S Jr, Hirsch E, Tanus-Santos JE, and Lacchini R. Relationship between asymmetric dimethylarginine, nitrite and genetic polymorphisms: Impact on erectile dysfunction therapy. *Nitric Oxide*. **71**: 44–51. 2017. [[Medline](#)] [[CrossRef](#)]
6. Baek JH, Zhang X, Williams MC, Hicks W, Buehler PW, and D'Agnillo F. Sodium nitrite potentiates renal oxidative stress and injury in hemoglobin exposed guinea pigs. *Toxicology*. **333**: 89–99. 2015. [[Medline](#)] [[CrossRef](#)]
7. Ribeiro MC, Bezerra TDS, Soares AC, Boechat-Ramos R, Carneiro FP, Vianna LMS, Faro LRF, Silva MVD, Vieira MP, Monteiro IO, and Ferreira VM. Hippocampal and cerebellar histological changes and their behavioural repercussions caused by brain ischaemic hypoxia experimentally induced by sodium nitrite. *Behav Brain Res*. **332**: 223–232. 2017. [[Medline](#)] [[CrossRef](#)]
8. Pottinger TG. Modulation of the stress response in wild fish is associated with variation in dissolved nitrate and nitrite. *Environ Pollut*. **225**: 550–558. 2017. [[Medline](#)] [[CrossRef](#)]
9. Fan AM, and Steinberg VE. Health implications of nitrate and nitrite in drinking water: an update on methemoglobinemia occurrence and reproductive and developmental toxicity. *Regul Toxicol Pharmacol*. **23**: 35–43. 1996. [[Medline](#)] [[CrossRef](#)]
10. Aly HA, Mansour AM, Abo-Salem OM, Abd-Ellah HF, and Abdel-Naim AB. Potential testicular toxicity of sodium nitrate in adult rats. *Food Chem Toxicol*. **48**: 572–578. 2010. [[Medline](#)] [[CrossRef](#)]
11. Shimizu T, Kosaka N, Murayama C, Tetsuka M, and Miyamoto A. Apelin and APJ receptor expression in granulosa and theca cells during different stages of follicular development in the bovine ovary: involvement of apoptosis and hormonal regulation. *Anim Reprod Sci*. **116**: 28–37. 2009. [[Medline](#)] [[CrossRef](#)]
12. Drazen DL, Klein SL, Burnett AL, Wallach EE, Crone JK, Huang PL, and Nelson RJ. Reproductive function in female mice lacking the gene for endothelial nitric oxide synthase. *Nitric Oxide*. **3**: 366–374. 1999. [[Medline](#)] [[CrossRef](#)]
13. Aschengrau A, Zierler S, and Cohen A. Quality of community drinking water and the occurrence of spontaneous abortion. *Arch Environ Health*. **44**: 283–290. 1989. [[Medline](#)] [[CrossRef](#)]
14. Schmitz JT. Methemoglobinemia—a cause of abortions? Preliminary report. *Obstet Gynecol*. **17**: 413–415. 1961.

- [Medline]
15. Ferreira-Dias G, Costa AS, Mateus L, Korzekwa AJ, Galvão A, Redmer DA, Lukasik K, Szóstek AZ, Woclawek-Potocka I, and Skarzynski DJ. Nitric oxide stimulates progesterone and prostaglandin E2 secretion as well as angiogenic activity in the equine corpus luteum. *Domest Anim Endocrinol.* **40**: 1–9. 2011. [Medline] [CrossRef]
 16. Kolb JP. Mechanisms involved in the pro- and anti-apoptotic role of NO in human leukemia. *Leukemia.* **14**: 1685–1694. 2000. [Medline] [CrossRef]
 17. Wu W, Gao X, Xu X, Luo Y, Liu M, Xia Y, and Dai Y. Saponin-rich fraction from *Clematis chinensis* Osbeck roots protects rabbit chondrocytes against nitric oxide-induced apoptosis via preventing mitochondria impairment and caspase-3 activation. *Cytotechnology.* **65**: 287–295. 2013. [Medline] [CrossRef]
 18. Lee TH, Lee MS, Huang CC, Tsao HM, Lin PM, Ho HN, Shew JY, and Yang YS. Nitric oxide modulates mitochondrial activity and apoptosis through protein S-nitrosylation for preimplantation embryo development. *J Assist Reprod Genet.* **30**: 1063–1072. 2013. [Medline] [CrossRef]
 19. Pinto CR, Paccamonti DL, Eilts BE, Short CR, and Godke RA. Effect of nitric oxide synthase inhibitors on ovulation in hCG-stimulated mares. *Theriogenology.* **58**: 1017–1026. 2002. [Medline] [CrossRef]
 20. Nath P, and Maitra S. Physiological relevance of nitric oxide in ovarian functions: An overview. *Gen Comp Endocrinol.* **279**: 35–44. 2019. [Medline] [CrossRef]
 21. Battaglia C, Salvatori M, Maxia N, Petraglia F, Facchinetti F, and Volpe A. Adjuvant L-arginine treatment for in-vitro fertilization in poor responder patients. *Hum Reprod.* **14**: 1690–1697. 1999. [Medline] [CrossRef]
 22. Kim KH, Oh DS, Jeong JH, Shin BS, Joo BS, and Lee KS. Follicular blood flow is a better predictor of the outcome of in vitro fertilization-embryo transfer than follicular fluid vascular endothelial growth factor and nitric oxide concentrations. *Fertil Steril.* **82**: 586–592. 2004. [Medline] [CrossRef]
 23. Hozayen WG, Mahmoud AM, Desouky EM, El-Nahass ES, Soliman HA, and Farghali AA. Cardiac and pulmonary toxicity of mesoporous silica nanoparticles is associated with excessive ROS production and redox imbalance in Wistar rats. *Biomed Pharmacother.* **109**: 2527–2538. 2019. [Medline] [CrossRef]
 24. Bouallegui Y, Ben Younes R, Oueslati R, and Sheehan D. Role of endocytotic uptake routes in impacting the ROS-related toxicity of silver nanoparticles to *Mytilus galloprovincialis*: a redox proteomic investigation. *Aquat Toxicol.* **200**: 21–27. 2018. [Medline] [CrossRef]
 25. D’Apolito M, Colia AL, Lasalvia M, Capozzi V, Falcone MP, Pettoello-Mantovani M, Brownlee M, Maffione AB, and Giardino I. Urea-induced ROS accelerate senescence in endothelial progenitor cells. *Atherosclerosis.* **263**: 127–136. 2017. [Medline] [CrossRef]
 26. Covantes-Rosales CE, Trujillo-Lepe AM, Díaz-Reséndiz KJG, Toledo-Ibarra GA, Ventura-Ramón GH, Ortiz-Lazareno PC, and Girón-Pérez MI. Phagocytosis and ROS production as biomarkers in Nile tilapia (*Oreochromis niloticus*) leukocytes by exposure to organophosphorus pesticides. *Fish Shellfish Immunol.* **84**: 189–195. 2019. [Medline] [CrossRef]
 27. Behrman HR, Kodaman PH, Preston SL, and Gao S. Oxidative stress and the ovary. *J Soc Gynecol Investig.* **8**(Suppl Proceedings): S40–S42. 2001. [Medline]
 28. El Mouatassim S, Guérin P, and Ménézo Y. Expression of genes encoding antioxidant enzymes in human and mouse oocytes during the final stages of maturation. *Mol Hum Reprod.* **5**: 720–725. 1999. [Medline] [CrossRef]
 29. Vega M, Carrasco I, Castillo T, Troncoso JL, Videla LA, and Devoto L. Functional luteolysis in response to hydrogen peroxide in human luteal cells. *J Endocrinol.* **147**: 177–182. 1995. [Medline] [CrossRef]
 30. Manova K, Huang EJ, Angeles M, De Leon V, Sanchez S, Pronovost SM, Besmer P, and Bachvarova RF. The expression pattern of the c-kit ligand in gonads of mice supports a role for the c-kit receptor in oocyte growth and in proliferation of spermatogonia. *Dev Biol.* **157**: 85–99. 1993. [Medline] [CrossRef]
 31. Manabe N, Goto Y, Matsuda-Minehata F, Inoue N, Maeda A, Sakamaki K, and Miyano T. Regulation mechanism of selective atresia in porcine follicles: regulation of granulosa cell apoptosis during atresia. *J Reprod Dev.* **50**: 493–514. 2004. [Medline] [CrossRef]